Mem. S.A.It. Vol. 81, 631

**Memorie** della

# Anisotropic transport processes in the chromosphere and overlying atmosphere

M. L. Goodman and F. Kazeminezhad

Advanced Technologies Group, West Virginia High Technology Consortium Foundation, 1000 Galliher Drive, Fairmont, WV 26554, USA, e-mail: mgoodman@wvhtf.org

**Abstract.** Energy flow and transformation in the solar atmosphere is a complex process. Fluxes of particle kinetic and electromagnetic energy flow in both directions through the photosphere, and are transformed into one another in the overlying atmosphere. Diffusive transport processes such as electrical and thermal conduction, and viscous and thermoelectric effects play a major role in determining energy fluxes and transformation rates. Almost the entire atmosphere is strongly magnetized, meaning that charged particle cyclotron frequencies significantly exceed their collision frequencies. This causes transport processes to be anisotropic, so they must be described by tensors in MHD models. Only models that include the relevant transport tensors can reveal the processes that create and maintain the chromosphere, transition region, and corona because only such models can accurately describe energy flow and transformation. This paper outlines the importance of anisotropic transport processes in the atmosphere, especially of anisotropic electrical conduction in the weakly ionized, strongly magnetized chromosphere, and presents MHD model evidence that anisotropic electrical conduction plays a major role in shock wave and Alfvén wave heating in the chromosphere. It is proposed that magnetization induced resistivity increases with height from the photosphere, exceeds the Spitzer resistivity $\eta_S$ near the height of the local temperature minimum, increases with height to orders of magnitude > $\eta_S$, and causes proton Pedersen current dissipation to be a major source of chromospheric heating.

**Key words.** MHD – shock waves – Sun: chromosphere – Sun: magnetic fields – Sun: photosphere – Stars: chromospheres

## 1. Introduction

The chromosphere is the mostly H I interface layer between the photosphere and corona. It merges into the transition region (TR) that is the lower boundary of the corona (e.g. Mariska 1992). All mass and energy that powers flares, coronal mass ejections, the solar wind, and the relatively steady coronal heating must flow from the photosphere through the chromosphere before it reaches the corona. The net radiative flux from the chromosphere is 10–100 times that from the overlying corona. Understanding the physics of the chromosphere is one of the keys to predicting Earth's space weather, and might be key to understanding coronal heating. A fundamental process in the weakly ionized, strongly magnetized chromosphere is the collisional coupling between charged particles and neutral gas. This coupling plays a major role in determining the

*Send offprint requests to*: M. L. Goodman flow and transformation of energy in the chromosphere, and along with electron-proton and proton-proton collisions in the upper chromosphere, TR, and lower corona affect the mass and energy flux into the corona.

The magnetization of a particle species $s$ is defined as $M_s = \omega_s \tau_s$, which is the product of the cyclotron frequency and total collision time. A species is said to be weakly (strongly) magnetized if $M_s < 1 (\gg 1)$. Charged particle-neutral gas collisions play a major role in determining the electrical conductivity tensor $\bar{\sigma}$ in the chromosphere where it is highly anisotropic due to the strong magnetization of protons and electrons, and, to a lesser extent, heavier ions. These collisions also determine $\bar{\sigma}$ in the underlying photosphere where it is largely isotropic due to weak magnetization. The parallel, Pedersen, and Hall conductivities that comprise $\bar{\sigma}$ govern resistive heating due to current flow parallel and perpendicular to the magnetic field $\mathbf{B}$. Although the Hall conductivity is non-dissipative, the ratio $\sigma_{\mathrm{H}}/\sigma_{\mathrm{P}}$ of the Hall to Pedersen conductivities controls the angle between the component $\mathbf{J}_{\perp}$ of the current density $\perp \mathbf{B}$, and the center of mass (CM) electric field $\mathbf{E}_{\mathrm{CM}} \equiv \mathbf{E} + (\mathbf{V} \times \mathbf{B})/c$. Here $\mathbf{E}, \mathbf{V}$, and $c$ are the electric field, CM velocity of the plasma, and the speed of light. Then the Pedersen current dissipation rate, $Q_{\mathrm{P}} = \mathbf{J}_{\perp} \cdot \mathbf{E}_{\mathrm{CM}}$ is partly controlled by the Hall conductivity. The ratio $\sigma_{\mathrm{H}}/\sigma_{\mathrm{P}}$ increases from values $\ll 1$ at the photosphere to values $\gg 1$ near the temperature minimum, and then rapidly decreases to values $\ll 1$ with increasing height into the chromosphere. This has a strong effect on $Q_{\mathrm{P}}$. The Hall conductivity can also couple orthogonal components of $\mathbf{B}$, and have strong dispersive effects, for example by splitting Alfvén waves into ion cyclotron and whistler waves, and by nonlinearly generating structure and heating on spatial scales down to the collisionless skin depths of electrons and protons.

The anisotropy of $\bar{\sigma}$ in the chromosphere partly determines $\mathbf{J}_{\perp}$, and so partly determines the magnetic Lorentz force $\mathbf{J}_{\perp} \times \mathbf{B}$, which is one of the drivers of flow. The resistive dissipation of Pedersen currents is regulated by the anisotropy of $\bar{\sigma}$, and acts to change this force. This effect might be important in controlling how the magnetic force lifts mass through the chromosphere into the corona (Leake & Arber 2006; Arber, Haynes & Leake 2007).

Alfvén waves can be strongly damped in the chromosphere by the dissipation of Pedersen currents driven by the $\mathbf{E}_{\mathrm{CM}}$ generated by the waves (De Pontieu, Martens & Hudson 2001; Leake, Arber & Khodachenko 2005; Kazeminezhad & Goodman 2006; Goodman 2010). The associated $Q_{\mathrm{P}}$ can be comparable to the chromospheric net radiative loss. It is proposed that the chromosphere is created and maintained by proton Pedersen current dissipation driven by the induction and convection electric fields of one or more MHD processes including smooth and shock waves, and quasi-steady flows (Goodman 2000, 2001, 2004a,b, 2010; Kazeminezhad & Goodman 2006; Goodman & Kazeminezhad 2010). This basic heating mechanism is unique to the weakly ionized, strongly magnetized chromosphere. This mechanism is not effective in the weakly ionized, underlying photosphere due to weak magnetization, and is not effective in the strongly magnetized, overlying corona due to strong ionization.

The effects of electron-proton (e-p) and proton-proton (p-p) collisions must also be included in an accurate description of transport processes in the atmosphere. Electron-proton collisions are important in determining the Pedersen resistivity $\eta_{\mathrm{P}}$ in the chromosphere at heights $z \lesssim 10^3$ km above the photosphere since $\eta_{\mathrm{P}} \propto M_{\mathrm{e}} M_{\mathrm{p}}$, and since $M_{\mathrm{e}}$ is mainly determined by e-p collisions in this region (Goodman 2004a). Electron-proton and p-p collisions completely determine transport processes in the TR and lower corona, and so play an important role in chromosphere-corona coupling. There p-p collisions dominate thermal conduction orthogonal to $\mathbf{B}$, e-p collisions determine thermal conduction parallel to $\mathbf{B}$, and e-p collisions determine thermoelectric current drive which is important in the TR (Goodman 1998) and in current sheets (Goodman 2005).

Transport processes play a major role in determining the radiation spectrum of plasmas for the following reason. The radiation spectrum is a sensitive function of temperature. This is shown by the presence of terms of the form $\exp(-E/k_{\mathrm{B}}T)$ that occur in radiative transfer models that determine ion densities, and atomic level populations and transition rates. Here $E$ is an energy that characterizes a given bound-bound, bound-free, or free-bound transition, and $k_{\mathrm{B}}$ is Boltzmann's constant. Then a small variation in $T$ may cause a large change in these terms, and hence in the radiation spectrum. Since $T$ is largely determined by transport processes such as resistive, viscous, and compressive heating rates, and electron, ion, and neutral particle thermal energy fluxes, it follows that transport processes play a major role in determining the radiation spectrum.

## 2. Ubiquity of anisotropic transport

With increasing height above the photosphere the plasma becomes strongly magnetized almost everywhere. This causes the transport tensors to become highly anisotropic. This means that electrical and thermal conductivities perpendicular to **B** differ from one another, and from those parallel to **B** by orders of magnitude. Similarly for the electron and ion viscosity tensors, and for the thermoelectric tensor that describes the generation of electric current and heat flux by a temperature gradient (e.g. Braginskii 1965; Chapman & Cowling 1970; Mitchner & Kruger 1973; Balescu 1988). This causes energy fluxes parallel and perpendicular to **B**, and their associated transformation rates to differ by orders of magnitude.

Different particles become magnetized at different heights. The degree of magnetization depends on the local magnetic field strength, particle densities, and temperature. For photospheric magnetic field strengths $\lesssim$ 100 G, for reasonable variations of the magnetic field strength with increasing height, and for typical density and temperature profiles (e.g. Fontenla, Avrett & Loeser 2002, , henceforth FAL) it follows that the electrons, protons, and minor ions become strongly magnetized within $\sim$ 300–1 000 km above the photosphere. The protons and minor ions tend to become strongly magnetized near the height of the FAL temperature minimum, with the electrons becoming magnetized a few hundred kilometers below this height. Then except in regions where the underlying photospheric magnetic field strength is $\ll$ 100 G, it is expected that magnetization induced, anisotropic transport processes play a major role in the heating, emission, and overall energetics of the atmosphere.

## 3. Examples

Neglecting thermoelectric and electron pressure gradient effects, which are probably not of major importance in the chromosphere, the Ohm's law for the chromosphere may be written as $\mathbf{E}_{\mathrm{CM}} = \eta_{\|}\mathbf{J}_{\|}+\eta_{\mathrm{H}}\mathbf{J}\times\hat{\mathbf{B}}+\eta_{\mathrm{P}}\mathbf{J}_{\perp}$ (Mitchner & Kruger 1973; Goodman 2004a,b). Here $\eta_{\|} = 1/\sigma_{\|}, \eta_{\mathrm{H}} = \eta_{\|}M_{\mathrm{e}} = B/(ecn_{\mathrm{e}})$, and $\eta_{\mathrm{P}} = (1 + \Gamma)\eta_{\|}$ are the parallel, Hall, and Pedersen resistivities. $\sigma_{\|}$, $n_{\mathrm{e}}$, and $e$ are the conductivity parallel to **B**, electron number density, and magnitude of the electron charge. $\Gamma = (\rho_n/\rho)^2 M_{\mathrm{e}} M_i$, where $\rho_n$ and $\rho$ are the neutral and total mass densities. $\hat{\mathbf{B}}$ is a unit vector parallel to **B**. **J** and $\mathbf{J}_{\|}$ are the total current density, and its component parallel to **B**. In the chromosphere $\eta_{\mathrm{P}} \gg \eta_{\|}$. In the photosphere and corona $\eta_{\mathrm{P}} \sim \eta_{\|}$. The Hall and Pedersen conductivities are related to the resistivities by $\sigma_{\mathrm{H}} = -\eta_{\mathrm{H}}/(\eta_{\mathrm{P}}^2 + \eta_{\mathrm{H}}^2)$, and $\sigma_{\mathrm{P}} = \eta_{\mathrm{P}}/(\eta_{\mathrm{P}}^2 + \eta_{\mathrm{H}}^2)$.

This Ohm's law describes a three fluid plasma of electrons, one species of ions representing protons and singly charged heavier ions, and one species of neutral gas representing H I and He I. The resistive heating rate corresponding to the Ohm's law is $Q = (J_{\|}^2 + (1 + \Gamma)J_{\perp}^2)/\sigma_{\|} \equiv Q_{\|} + Q_P$, where $Q_{\|} = J_{\|}^2/\sigma_{\|}$. For a fully ionized plasma, $\Gamma = 0$. The last two terms on the right hand side of the Ohm's law are the Hall and Pedersen electric fields. They play a major role in chromospheric heating and dynamics, mainly due to the fact that the conditions $\Gamma \gg 1$ and $M_{\mathrm{e}} \gg 1$ hold in the chromosphere. Under these conditions it is found that $Q_{\mathrm{P}}$ is many orders of magnitude larger than $Q_{\|}$, and can be comparable to the chromospheric heating rate (e.g. Goodman 2000, 2001, 2004a,b; Kazeminezhad & Goodman 2006).

### 3.1. Heating in shock waves

Kazeminezhad & Goodman (2006) present 1.5 D MHD simulations of fast magnetoacoustic type waves generated in the photosphere that steepen into shock waves ~ 370 km above the photosphere, and propagate upward through the chromosphere. The resolution of the simulations is 1 km, the initial state is the FAL CM 1 D hydrostatic atmosphere, and a horizontal magnetic field $B_x(z, t = 0) = B_0 \exp(-\alpha \int_0^z \mathrm{d}u/(2L(u)))$. Here $L$ is the local ideal gas pressure scale height computed using the FAL temperature profile and average local particle mass, $\alpha$ is a constant chosen so $B_x$ does not exceed a few tens of G in the upper chromosphere, $t$ is time, and $z$ is height above the photosphere at $z = 0$. The Ohm's law in §3 is used in the model. The temperature and particle density profiles used to compute the collision frequencies in the Ohm's law are FAL profiles, and hence are independent of time, although the MHD equations evolve the total density and the ideal gas temperature $T = p/nk_\mathrm{B}$ in time, where $p$ and $n$ are the total pressure and number density. The source terms in the thermal energy equation are the resistive dissipation rate $Q$, which for this model reduces to $Q_\mathrm{P}$, and the compressive heating rate $Q_\mathrm{c} = -p\nabla \cdot \mathbf{V}$, which may be positive or negative corresponding to heating by compression or cooling by rarefaction. The simulation is driven by a magnetic field at the photosphere given by $B_x(0, t) = B_0 + \delta B_x \sin(2\pi t/T)$, with $B_0 = 500$ G, $\delta B_x = 250$ G, and $T = 30$ seconds. The simulation is run for 200 seconds, generating a train of 6 shock waves, shown in Fig. 1, extending from just below the FAL temperature minimum near $z = 500$ km, up to the base of the TR. The shock layer thicknesses are ~ 10–20 km.

Figure 2 shows how the magnetization induced component of $\eta_\mathrm{P}$, given by $\Gamma\eta_\parallel$ maintains the resistivity of the chromosphere at values orders of magnitude larger than $\eta_\parallel$. This causes $Q$ to be orders of magnitude larger than it is in the absence of magnetization effects. This also causes the thickness of the shock layers to be larger than they are in the absence of magnetization effects. In the ideal MHD limit of $\eta_\mathrm{P} \to 0$ the shock layer thickness is zero. It is conjectured the magnetization induced resistivity has a significant effect on $Q_\mathrm{c}$. The integrals of $Q$ and $Q_\mathrm{c}$ over the height range of the shock wave train ($370 \leq z(\mathrm{km}) \leq 2039$) are $F = 4.6 \times 10^6$ ergs cm$^{-2}$ s$^{-1}$ and $F_\mathrm{c} = 1.24 \times 10^9$ ergs cm$^{-2}$ s$^{-1}$. This suggests that compressive heating dominates resistive heating in shock waves.

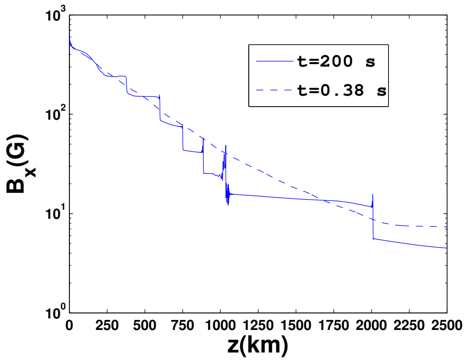


**Fig. 1.** Magnetic field vs. height at the beginning and end of the simulation.

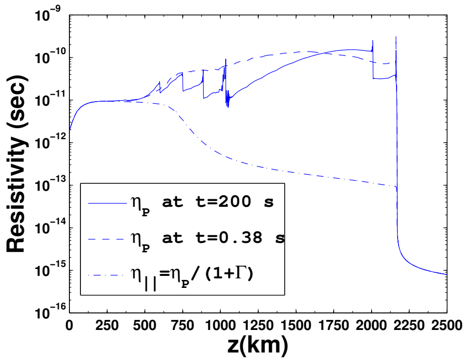


**Fig. 2.** Pedersen resistivity $\eta_\mathrm{P}$ vs. height at the beginning and end of the simulation, and parallel resistivity $\eta_\parallel$ vs. height. $\eta_\parallel$ is independent of time since FAL data is used to compute it.

Figures 3 and 4 show the resistive and compressive heating rates per unit mass, $Q_m = Q/\rho$ and $Q_{cm} = Q_\mathrm{c}/\rho$. Essentially all resistive and compressive heating in the region $z \geq 370$ km occurs in the shock layers. The inter-shock regions are in a state of rarefaction. The average of $Q_m$ over the shock wave train is 2.5 ×

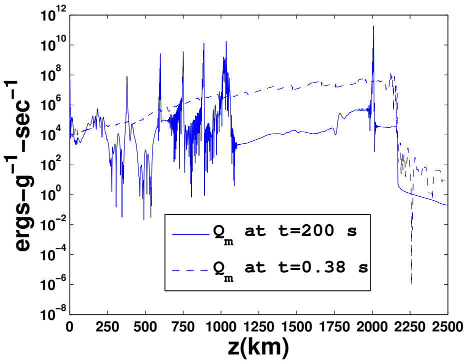


**Fig. 3.** Resistive heating rate per unit mass vs. height at the beginning and end of the simulation.

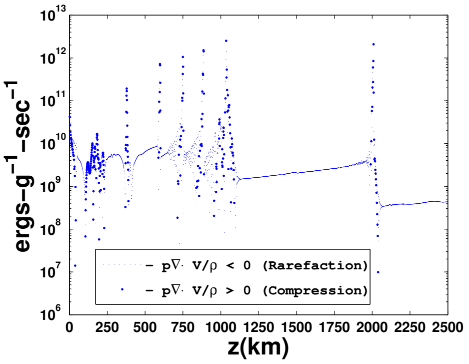


**Fig. 4.** Compressive heating rate per unit mass vs. height at the end of the simulation.

$10^8$ ergs $g^{-1}$ $s^{-1}$. The averages of the positive and negative values of $Q_{cm}$ over the shock wave train are $1.25 \times 10^{11}$ ergs $g^{-1}$ $s^{-1}$, and $-1.21 \times 10^{10}$ ergs $g^{-1}$ $s^{-1}$. The average of all values of $Q_{cm}$ over the shock wave train is $1.29 \times 10^8$ ergs $g^{-1}$ $s^{-1}$. The heating rates per unit mass appear to be suppressed by the mass density that evolves to values ≫ FAL values.

### 3.2. Heating by driven Alfvén waves

Extending work by De Pontieu, Martens & Hudson (2001) and Leake, Arber & Khodachenko (2005) on Alfvén wave dissipation in the chromosphere by Pedersen current dissipation, Goodman (2010) develops a 1.5 D, analytically solvable MHD model for

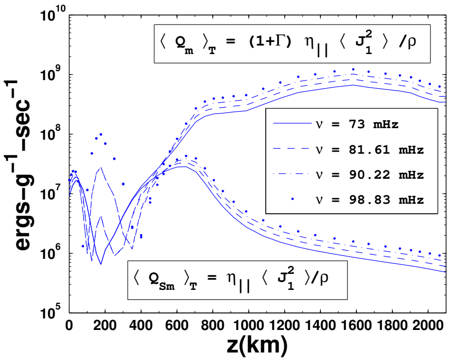


**Fig. 5.** Period averaged total and Spitzer heating rates per unit mass vs. height for 4 values of the driving frequency. The spatial average of the total heating rate over the height range $1000 \leq z(\mathrm{km}) \leq 2100$ increases with frequency from $4.74 \times 10^8$ to $8.7 \times 10^8$ ergs $g^{-1}$ $s^{-1}$. The corresponding range of the chromospheric resistive heating flux, which is the integral of $Q$ over $500 \leq z(\mathrm{km}) \leq 2100$ is $\sim 5 - 7.8 \times 10^6$ ergs $cm^{-2}$ $s^{-1}$. Here $B_\Gamma(0) = 500$ G, and $B_{x1}(0,0) = 140$ G. If $B_z$ and $\omega$ are fixed then $Q$ and $Q_m$ are $\propto B_{x1}^2(0,0) B_\Gamma^2(0)$ when $1 + \Gamma \sim \Gamma$.

estimating the conditions under which proton Pedersen current dissipation driven by the $\mathbf{E}_{CM}$ of monochromatic, linear, non-plane Alfvén waves can be a significant source of chromospheric heating, and the conditions under which the Poynting flux of these waves in the upper chromosphere can be a significant source of energy for the corona. Boundary conditions are given at the photosphere to determine the perturbation amplitudes as functions of height from the photosphere to the base of the TR. The background state is FAL with $B_z = 200$ G, and uses FAL profiles and an ad hoc magnetic field strength $B(z) \equiv B_\Gamma(0) \exp(-\alpha \int_0^z d\gamma/(2L(\gamma))$, similar to the magnetic field in the previous section, to determine the conductivity tensor. The Ohm's law in §3 is used in the model. Let $B_{x1}(0,0)$ and $\omega = 2\pi/T = 2\pi\nu$ be the amplitude of the perturbation of the $x$ component of the magnetic field at $z = t = 0$, and the driving frequency. The solution to the model is determined once $B_z$, $B_\Gamma(0)$, $B_{x1}(0,0)$, and $\omega$ are given.

The model predicts $Q(z,t)$, the Poynting flux $S_z(z,t)$, and the perturbation amplitudes

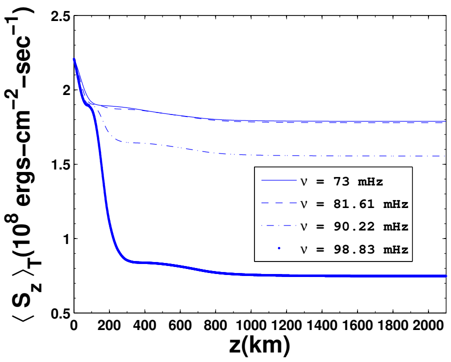


**Fig. 6.** Period averaged vertical Poynting flux vs. height for four values of the driving frequency. Here $B_\Gamma(0) = 500$ G, and $B_{x1}(0,0) = 140$ G. If $B_\Gamma(0)$, $B_z$, and $\omega$, are fixed, then $\langle S_z \rangle_T \propto B^2_{x1}(0,0)$.

$B_{x1}(z,t)$, $B_{y1}(z,t)$, $V_{x1}(z,t)$, $V_{y1}(z,t)$. Figure 5 shows several solutions for the period average, denoted by $\langle\rangle_T$, of $Q_m$ and its Spitzer component $Q_{Sm}$ as defined in the figure. The Spitzer component is insignificant compared with the magnetization induced component $\propto \Gamma \propto B^2_\Gamma(0)$. The indicated spatial averages of $Q_m$, and the total chromospheric heating fluxes are comparable to observationally inferred values $\sim 10^9$ ergs g$^{-1}$ s$^{-1}$, and $\sim 5 - 10 \times 10^6$ ergs cm$^{-2}$ s$^{-1}$ (e.g. Withbroe & Noyes 1977; Anderson & Athay 1989).

Figure 6 shows the Poynting fluxes corresponding to Fig. 5. The flux in the upper chromosphere is $\sim 10$ times larger than the total coronal energy loss over active regions. For this case the waves dissipate enough energy to balance a large fraction of the net radiative loss from the chromosphere, and retain more than enough Poynting flux at the base of the TR to balance coronal energy losses.

## 4. Conclusions

The solar atmosphere is divided into 3 transport regions: the weakly ionized, weakly magnetized photosphere; the weakly ionized, strongly magnetized chromosphere; and the strongly ionized, strongly magnetized corona. The magnetization of protons and electrons combined with proton-H I collisions cause proton Pedersen current dissipation to be a major source of chromospheric heating.

*Acknowledgements.* The authors thank the workshop staff for an excellent program. This work was supported by NSF grant ATM-0650443.

## References


Anderson, L. S. & Athay, R. G. 1989, ApJ, 346, 1010

Arber, T. D., Haynes, M. & Leake, J.E. 2007, ApJ, 666, 541

Balescu, R. 1988, in Transport Processes in Plasmas, Vol. 1 (North Holland, New York)

Braginskii, S. I. 1965, in Transport Processes in a Plasma, Reviews of Plasma Physics Vol. 1 (Consultants Bureau, New York), 205

Chapman, S. & Cowling, T. J. 1970, in The Mathematical Theory of Non - Uniform Gases, ed. Chapman, S. & Cowling, T. G. (Cambridge University Press, Cambridge)

De Pontieu, B., Martens, P. C. H. & Hudson, H. S. 2001, ApJ, 558, 859

Fontenla, J. M., Avrett, E. H. & Loeser, R. 2002, ApJ, 572, 636

Goodman, M. L. 1998, ApJ, 503, 938

Goodman, M. L. 2000, ApJ, 533, 501

Goodman, M .L. 2001, Space Sci. Rev., 95, 79

Goodman, M. L. 2004a, A&A, 416, 1159

Goodman, M. L. 2004b, A&A, 424, 691

Goodman, M. L. 2005, ApJ, 632, 1168

Goodman, M. L. 2010, A&A, submitted

Goodman, M. L. & Kazeminezhad, F. 2010, ApJ, 708, in press

Kazeminezhad, F. & Goodman, M. L. 2006, ApJS, 166, 613

Leake, J. E., Arber, T. D. & Khodachenko, M.L. 2005, A&A, 442, 1091

Leake, J. E. & Arber, T. D. 2006, A&A, 450, 805

Mitchner, M. & Kruger, C. H. 1973, in Partially Ionized Gases (Wiley, New York)

Mariska, J.T. 1992, in The Solar Transition Region (Cambridge University Press, New York)

Withbroe, G. L. & Noyes, R. W. 1977, ARA&A, 15, 363